COLD SPRING HARBOR
Molecular Case Studies

RESEARCH REPORT

Case report: *EWSR1-TFCP2* in an adolescent represents an extremely rare and aggressive form of intraosseous spindle cell rhabdomyosarcomas

Agnesa V. Panferova,[1] Kseniya Yu. Sinichenkova,[1] Meriam Abu Jabal,[1] Natalia Yu. Usman,[1] Anastasya S. Sharlai,[2] Vitalii Yu. Roshchin,[2] Dmitry M. Konovalov,[2] and Alexander E. Druy[1]

[1]Laboratory for Molecular Oncology, [2]Pathology Department, Dmitry Rogachev National Medical Research Center of Pediatric Hematology, Oncology and Immunology, Ministry of Health, Moscow, 117198 Russia

Abstract The World Health Organization (WHO) Classification of Tumors of Soft Tissue and Bone subdivides rhabdomyosarcomas (RMSs) into alveolar, embryonal, pleomorphic, and spindle cell RMSs. Advances in molecular genetic diagnostics have made it possible to identify new RMS subgroups within traditional morphological entities. One of these subgroups comprises rare tumors characterized by epithelioid and spindle cell morphology, a highly aggressive clinical course with pronounced tendency to intraosseous growth, and the presence of pathognomonic recurring genetic aberrations—chimeric genes/transcripts *EWSR1::TFCP2*, *FUS::TFCP2*, or *MEIS1::NCOA2*. Starting from 2018, only 26 reported cases of RMS have been assigned to this subgroup. The rarity of such tumors hampers their correct diagnostics for both anatomic pathologists and molecular oncologists. Here, we describe a clinical case of intraosseous spindle cell RMSs expressing the *EWSR1::TFCP2* fusion gene, encountered for the first time in our practice, in a 16-yr-old female patient presenting with mandibular lesion. The diagnostic process took considerable time and involved RNA sequencing—a high-throughput method of molecular genetic research. The tumor was extremely aggressive, showing resistance to polychemotherapy, radiation therapy, and crizotinib-targeted therapy, with the fatal outcome.

[Supplemental material is available for this article.]

Corresponding author: agnesa.panferova@fccho-moscow.ru

Ontology term: rhabdomyosarcoma

Published by Cold Spring Harbor Laboratory Press

doi:10.1101/mcs.a006209

INTRODUCTION

Rhabdomyosarcomas (RMSs) account for more than one-half of pediatric soft tissue tumors (Emami et al. 2017). Spindle cell RMSs with primary intraosseous localization are extremely rare, which hampers their early accurate diagnosis (Watson et al. 2018; Agaram et al. 2019; Chrisinger et al. 2020; Le Loarer et al. 2020; Koutlas et al. 2021). Meanwhile, these tumors are aggressive, highly metastatic, and >60% lethal (Chrisinger et al. 2020; Koutlas et al. 2021). A recently recognized molecular subgroup of *EWSR1*/*FUS*/*MEIS1*::*TFCP2*/*NCOA2*-fused spindle cell RMSs (WHO Classification 2020) are typically presenting with primary intraosseous lesions. Here, we report a case of *EWSR1::TFCP2*-positive RMS with an outstandingly

aggressive clinical course identified with this subgroup. Our experience complements the current knowledge for these rare tumors and facilitates their better understanding. Furthermore, we suggest the early implementation of the molecular techniques in parallel with the conventional histopathology to the diagnostic algorithm of intraosseous neoplasms. Apart from the enhanced personalized patient management, another important mission of the early molecular diagnostics is enrollment. The emerging status of TFCP2 as a plausible therapeutic target will require extensive clinical verification on cohorts with timely diagnosed tumors harboring corresponding aberrations (Willoughby et al. 2020). ALK overexpression observed in the majority of reported intraosseous RMSs implicates potential efficacy of ALK inhibitors (Lewin et al. 2019; Le Loarer et al. 2020). However, clinical data on the use of ALK inhibitors in RMSs are quite limited and the results are controversial. Here we report on an attempt to use the ALK inhibitor crizotinib that proved unsuccessful.

RESULTS

Clinical Presentation

A 16-yr-old girl consulted a dentist about pain and swelling of the lower jaw on the left side. Computed tomography (CT) showed a 64-mm × 18-mm × 44-mm unossified mass in the mandible. A preliminary diagnosis of fibrosarcoma (from a biopsy) was revised by histological assessment of the resected tumor specimen after single-stage subtotal mandibulectomy and reconstruction with endoprosthesis. As the tumor was positive for SATB2, negative for CD34, desmin, MSA, S100, SMA, and weakly stained with anti-pan cytokeratin antibody (HCK AE1/AE3), the diagnosis was revised as fibroblastic osteosarcoma. The Ki-67 index was 50%. Postoperative magnetic resonance imaging (MRI) showed neither residual tumor nor metastases. However, the patient presented with local relapse even before the commencement of polychemotherapy (PChT, the EURAMOS-2007 protocol for patients with osteogenic sarcoma). MRI performed after the first block of PChT (doxorubicin, cisplatin) showed tumor growth spreading to the maxilla, with metastatic involvement of lymph nodes in the neck, C1–C2 vertebrae, and the iliac wing on the left (Fig. 1). Thus, the tumor progression occurred 2 mo after primary diagnosis.

A follow-up histological assessment revealed solid tumor, invading beyond the mandibular cortex, lacking osteoid, composed of spindle-shaped and polymorphic cells showing extremely high mitotic activity with atypical mitotic figures, arranged in short multidirectional fascicles. Given the characteristic morphology, complemented with expression of vimentin, desmin, H3K27me3, and focal expression of myogenin (Myf4), HCK AE1/AE3, SATB2, and

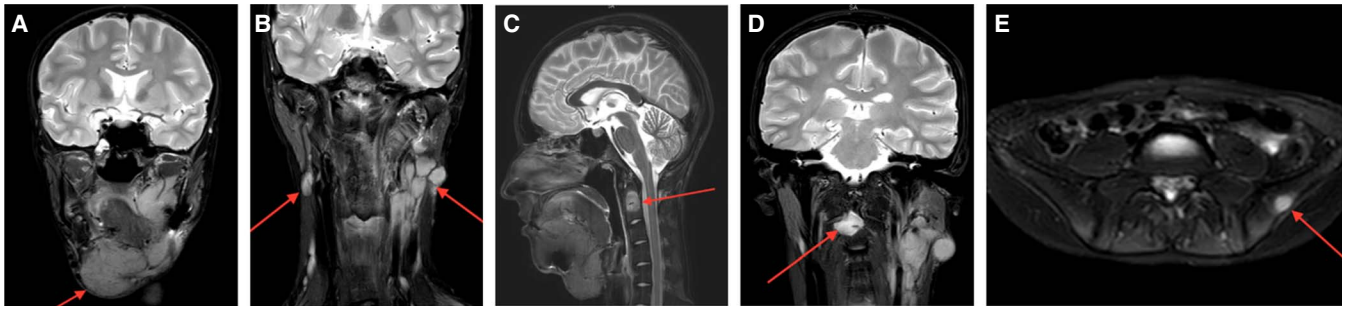

Figure 1. T2-weighted contrast-enhanced magnetic resonance imaging (MRI) scans of head and neck soft tissues (*A–D*) and pelvic bones (*E*) with arrows indicating primary and metastatic foci (*A*,*B–E*, respectively).

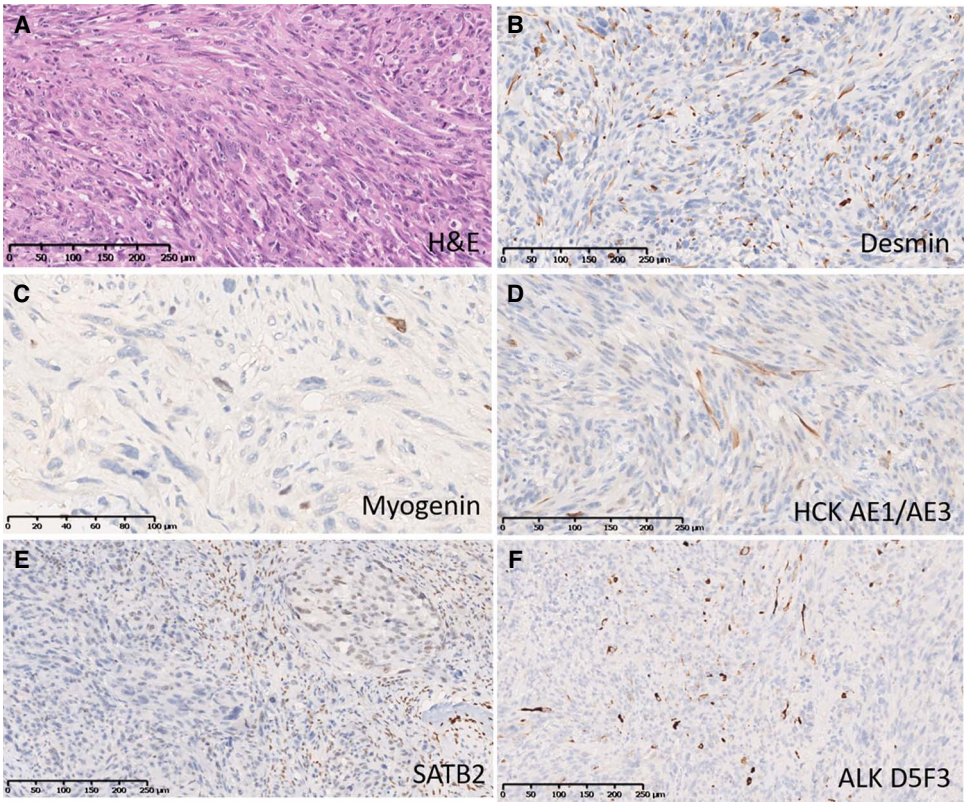

Figure 2. (*A*) Hematoxylin and eosin (H&E) 200×. The tumor grows in short fascicles intersecting at various angles, composed of large spindle or polymorphic cells with a moderate amount of weakly eosinophilic cytoplasm. The ovoid or irregularly shaped nuclei are positioned eccentrically and contain clumped chromatin, occasionally hyperchromatic, with one to three nucleoli. The mitotic activity is very high, with atypical mitotic figures. The moderately developed stroma contains ubiquitously distributed collagen fibers and a diffuse capillary network. Bone trabeculae, partially destroyed, are encountered within the tumor mass. Immunohistochemical examination reveals positivity for desmin (*B*), along with focal positivity for myogenin, HCK AE1/AE3, SATB2, and ALK D5F3 (*C–F*, respectively).

ALK D5F3 demonstrated by immunohistochemistry (Fig. 2; Supplemental Figs. 2–4), the diagnosis was revised to rhabdomyosarcoma, formally meeting the criteria for an embryonal variant.

With regard to the updated morphological diagnosis, the management strategy was switched to the CWS-2009 regimen for patients with distant metastases. With the first block of PChT (ifosfamide, vincristine, and dactinomycin), the primary focus showed no dynamics, but the distant metastasis in the iliac wing on the left grew. By the end of the second block (carboplatin, etoposide, and doxorubicin), progression of the disease was evident (4.5 mo after primary diagnosis), as the mass spread from corpus and ramus of the mandible and increased in volume by 39%.

Genomic Analyses

With consideration for the aggressive course of the disease and complete failure of first-line therapy, high-throughput DNA sequencing with a QIAseq custom panel comprising biomarkers of solid tumors in children (QIAGEN) was implemented for the molecular profile

Table 1. Variant table

Gene	Chromosome	HGVS DNA reference	HGVS protein reference	Variant type	Predicted effect	dbSNP/dbVar ID	Genotype	Interpretation[a]
TP53	17	c.559 + 1G > A	–	Substitution	Affecting splicing	rs1131691042	Heterozygous	Level IB

[a]Association for Molecular Pathology (AMP)/American Society of Clinical Oncology (ASCO)/College of American Pathologists (CAP) guidelines AMP/ASCO/CAP Variant Evidence Guidelines.

characterization and diagnosis verification (Supplemental Tables 1 and 2). The study revealed a *TP53* c.559 + 1G > A (Table 1) somatic variant (reference transcript ENST0000 0269305.4) of high prognostic significance (the AMP/ASCO/CAP level IB) (Li et al. 2017).

However, the atypical clinical patterns with intraosseous localization and the lack of response to PChT implicated the involvement of other molecular-genetic determinants, thus justifying the use of high-throughput RNA sequencing (TruSeq RNA Exome, Illumina). The analysis of RNA extracted from the primary formalin-fixed, paraffin-embedded (FFPE) tumor tissue revealed a *EWSR1::TFCP2* chimeric transcript (Table 2; Fig. 3; Supplemental Table 3) of the recurrent type encountered in spindle cell RMSs (Chrisinger et al. 2020).

Since 2020, RMSs harboring *EWSR1::TFCP2, FUS::TFCP2*, or *MEIS1::NCOA2* fusions, sharing characteristic clinical, morphological, immunohistochemical, and molecular features, have been assigned to a distinct subgroup in WHO Classification 2020 termed "Rhabdomyosarcomas with *TFCP2/NCOA2* fusions." The *EWSR1* rearrangement was additionally verified by fluorescence in situ hybridization (Fig. 4) confirming the diagnosis of intraosseous spindle cell RMS expressing *EWSR1::TFCP2* chimeric transcript.

Treatment Outcomes

The ultimate attempt to stop the tumor expansion was made with radiation therapy applied to the area of the primary focus and metastatic foci in the C1–C2 vertebrae and administered in single focal doses of 1.8 Gy to a total focal dose of 54 Gy. As the radiation therapy failed to suppress the continued tumor growth in the primary focus area, it was decided to escalate the intensity to 1.6 Gy focal doses twice a day, amounting to the same total focal dose of 54 Gy. A combination of vincristine, irinotecan, and temozolamide was used as systemic chemotherapy. With regard to the focal expression of ALK by the tumor, the regimen was complemented with crizotinib as a salvage treatment. Crizotinib was administered in dose 180 mg/m^2 or 250 mg *per os* daily for 10 d until the subsequent disease progression. No crizotinib-related side effects were observed. Notwithstanding these efforts, the patient's clinical condition steadily worsened, and neither primary nor metastatic foci responded to the treatment. Because of exhaustion of therapeutic options, the patient was declared incurable and discharged to palliative care after 6.5 mo after primary diagnosis. Five months later, the patient died because of the cancer progression. The time line is presented as the Supplemental Figure 1.

Table 2. Fusion transcript variant

Sample name	Million aligned reads	Mb aligned bases	Fusion gene	Left breakpoint	Right breakpoint	Coverage bases gene 1	Coverage bases gene 2
RNA5	11.8	959	*EWSR1:: TFCP2*	Chr 22: 29278216:+	Chr 12: 51118772:+	823	854

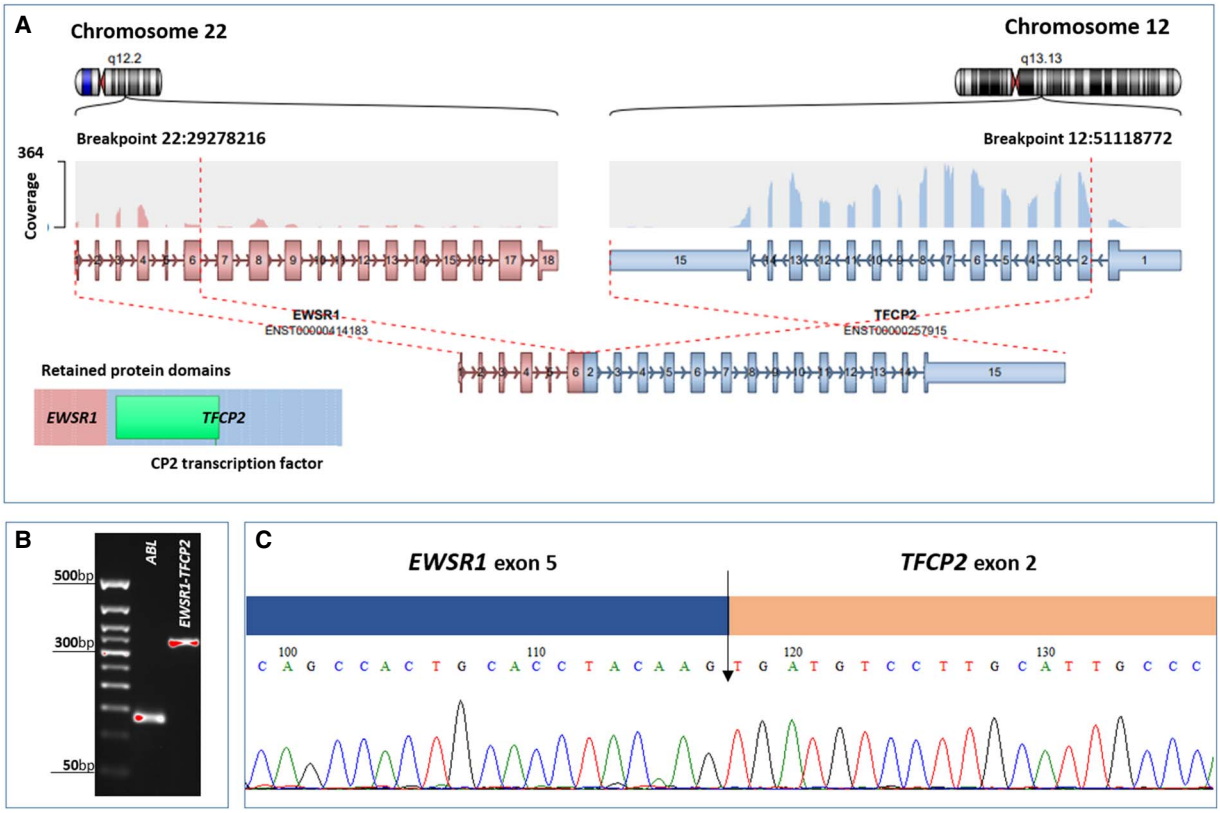

Figure 3. Identification of the *EWSR1::TFCP2* fusion transcript. (*A*) Schematic representation (Arriba v2.1.0) of the chimeric mRNA identified by high-throughput sequencing of RNA isolated from paraffin-embedded tissue, with the TruSeq RNA Exome kit (Illumina) used for the sequencing library construction. The sequencing was run in paired-end mode (2 × 100) on a NextSeq500 instrument (Illumina); the alignment to a reference human genome hg38 was performed in a Dragen RNA pipeline (v3.6.3, Illumina). (*B*) Validation of the finding: agarose gel with reverse transcription–polymerase chain reaction products for *EWSR1:TFCP2* chimeric product and *ABL* as a reference transcript, 340 and 130 bp, respectively. (*C*) Sanger sequencing chromatogram for the chimeric product, showing fusion between *EWSR1* exon 5 ENST00000414183.6 and *TFCP2* exon 2 ENST00000257915.9.

DISCUSSION

Malignant neoplasms sharing their origin with skeletal muscles (RMSs) are classified in WHO Classification of Soft Tissue and Bone Tumors 2020 into embryonal, alveolar, pleomorphic, and spindle cell RMSs. Of those, spindle cell RMSs represent the least prevalent and most heterogeneous morphological entity with diverse molecular driver events, including *VGLL2*:*NCOA2*/*CITED2* fusion-related congenital/infantile spindle cell RMSs, *MYOD1*-mutated spindle cell/sclerosing RMSs, and the intraosseous spindle cell RMSs with *TFCP2*/*NCOA2* rearrangements. Accurate differentiation between molecular subgroups of spindle cell RMSs is important because of their strong clinical significance.

Spindle cell RMSs harboring *TFCP2*/*NCOA2* rearrangements have been distinguished as an entity since 2018. Initially characterized by Watson et al. (2018), this molecular subgroup comprises a total of 26 cases worldwide reported by the time of this writing (Chrisinger et al. 2020; Koutlas et al. 2021). The primary lesions emerge in skull bones (predominantly in the maxilla or the mandible) and much less typically in other skeletal areas (pelvic bones, spine,

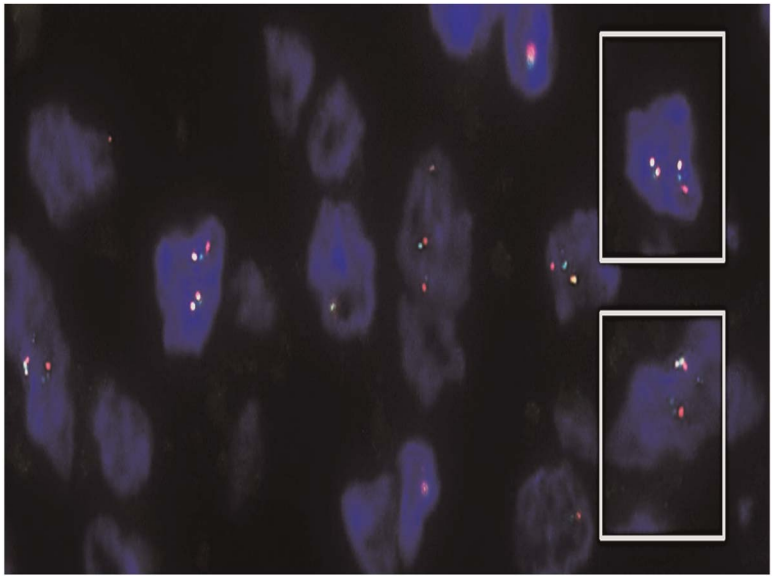

Figure 4. Fluorescence in situ hybridization. A 600× image shows tumor cell nuclei with clumpy chromatin, most of them containing a couple of fused signals designated 2F, corresponding to the intact *EWSR1* (no rearrangement). Small clusters of cells containing a combination of fused and broken apart signals indicating a translocation involving *EWSR1* (1F1R1G) are scattered over the whole section area. The image was produced using ZytoLight SPEC EWSR1 Dual Color Break Apart Probe, with red and green fluorochromes corresponding to proximal and distal regions of *EWSR1* (22q12), respectively.

etc.) or abdominal/inguinal soft tissues (Le Loarer et al. 2020). Gross examination reveals solid tissue with residual bone trabeculae and signs of vascular invasion, with a capacity to invade soft tissues. The age at onset varies (11–86 yr), with the median in the third decade of life. The estimated gender-specific morbidity shows female prevalence (~1.7:1) (Chrisinger et al. 2020). Histological assessment reveals layers/cords of epithelioid/spindle tumor cells with eosinophilic cytoplasm. The large nuclei are rounded or elongated (in rare cases—pleomorphic) and contain clumpy chromatin, occasionally hyperchromatic, with prominent nucleoli; the cytoplasm is scanty to moderate. Some of the tumors show round cell morphology. True rhabdomyoblasts may be missing. The moderately developed stroma is sclerotic and partially hyalinized. The positivity for MYOD1 and desmin, and to a lesser degree for myogenin, is revealed by immunohistochemistry. In addition, the tumors are cytokeratin-positive and may also express auxiliary markers ALK and S100. The intraosseous spindle cell RMS with *TFCP2* rearrangements are extremely aggressive tumors with the most adverse prognosis (Agaram et al. 2019; Chrisinger et al. 2020; Le Loarer et al. 2020; Koutlas et al. 2021).

The current case of *EWSR1::TFCP2*-fused RMS fairly complies with this description in terms of morphology and immunohistochemistry, and it showed the most aggressive clinical course. The involved gene *EWSR1* (22q12.2) encodes a multifunctional RNA-binding protein related to *FUS* and *TAF15* (Lee et al. 2019). The continuous transcriptional activity of the *EWSR1* locus in certain tissues is associated with high risks of somatic chromosome rearrangements. Fusion of chromosome fragments may produce a chimeric oncogene comprising the 5′ region of *EWSR1* and the 3′ region of another gene (e.g., *TFCP2*). Such variants act as transcription regulators with impaired specificity (Lindén et al. 2019) and promote oncogenesis. The *EWSR1*/*FUS* rearrangements are pathognomonic for certain soft tissue and bone neoplasms including Ewing sarcoma, desmoplastic small round cell tumor, and

sclerosing epithelioid fibrosarcoma. As a particular chimeric variant may serve an unambiguous marker of a particular tumor type, identification/exclusion of such rearrangements is indispensable for the diagnosis.

The *TFCP2* gene (12q13.12) contributes to the 3′ region of the *EWSR1::TFCP2* and *FUS::TFCP2* chimeric transcripts. *TFCP2* encodes a transcription factor called α-globin transcription factor CP2 (*a.k.a.* late SV40 factor, LSF) considered as a prospective molecular target in certain tumors. Synthetic small inhibitory molecules termed factor quinolinone inhibitors (FQIs) interact with LSF and restrict its DNA-binding capacity. Sustained anti-tumor activity of FQIs without observable toxic effects was demonstrated in several preclinical models. According to functional studies, targeted inhibition of LSF with small molecules or microRNA effectively interferes with the mitotic cycle, promoting cell death or cell senescence (Willoughby et al. 2020). These findings support the emerging status of LSF as an actionable target, of vital significance under the lack of response to standard protocols. Apart from that, focal expression of ALK by an intraosseous tumor implicates potential efficacy of ALK inhibitors; however, clinical data on the use of ALK inhibitors in RMSs are quite limited and the results are controversial (Lewin et al. 2019; Le Loarer et al. 2020; Lee et al. 2021). Here we describe an attempt to use the ALK inhibitor crizotinib as a salvage therapy that proved unsuccessful.

Because the intraosseous *EWSR1::TFCP2*-fused tumors are rare, they represent a major diagnostic challenge, particularly given the extensive list of competing possibilities for differential diagnosis. This flaw is crucial, as a delay with accurate diagnosis enabling correct choice of the treatment strategy most adversely impacts the prognosis. The diagnostic algorithm can be improved by explicitly expanding the scope of clinical situations for which the morphological/immunohistochemical assessment must be closely supported by comprehensive molecular genetic tests performed on an urgent basis.

METHODS

Written informed consent was obtained from the parents of the individual for participation in the study and the publication. All procedures performed were in accordance with the ethical standards of the institutional and national research committee. The study was approved by the Institutional Review Board of the Dmitry Rogachev National Medical Research Center of Pediatric Hematology, Oncology, and Immunology.

In this study, all genetic and fluorescence in situ hybridization (FISH) analyses were performed using primary FFPE tumor tissue.

FISH studies were performed using FFPE specimens sectioned into 4-µm-thick tissue sections. Briefly, after dewaxing and hydration, the sections were immersed in Pretreatment Solution (Agilent Technologies) for 15 min at 95°C–100°C. After digestion in RTU pepsin (Agilent Technologies) 15 min at room temperature (RT), the sections were washed in Wash Buffer (Agilent Technologies) for 5 min at RT, then dehydrated in an ethanol series (70%, 85%, and 100%) for 1 min each at RT and air dried. The slides were hybridized with 10 µL SPEC EWSR1 Dual Color Break Apart FISH Probe (ZytoVision). Probes were applied to the tissue slide, coverslipped, and sealed with rubber cement. Denaturation was conducted for 5 min at 78°C and hybridized 12–18 h at 37°C in Hybridizer (Dako). Posthybridization washing was performed in Stringent Wash Buffer (Agilent Technologies) at a preheated temperature of 74°C. Air-dried slides were counterstained using Fluorescence Mounting Medium (Agilent Technologies) and coverslipped. The slides were observed using a fluorescence microscope with appropriate filters, and the resulting images were captured using a charge-coupled-device camera (Olympus BX63).

High-throughput DNA sequencing: QIAseq (QIAGEN) custom panel comprising biomarkers of solid tumors in children (*ATM, ALK, APC, ATRX, BRAF, BCOR, BRCA1, BRCA2, CDKN2A, CDKN2B, CIC, CREBBP, CTNNB1, DICER1, DROSHA, EGFR, FBXW7, FGFR1, HRAS, IDH1, IDH2, KDR, KIT, KRAS, MAP2K1, MAP2K2, MYOD1, MET, MSH6, MSH2, MLH1, NF1, NOTCH1, NRAS, PDGFRA, PDGFRB, PIK3CA, POLD, POLE, PTCH1, PTEN, PTPN11, RB1, ROS1, RET, SMARCA4, SMARCB1, SUFU, SMO, TSC1, TERT, TP53, TSC2, WT1, H3F3A, HISTH3B*). Paired-end (2 × 150 bp) run was performed on the MiSeq instrument (Illumina) with a mean read depth 488 and subsequent analysis by alignment to a reference human genome hg37 in a GeneGlobe pipeline (QIAGEN).

Chimeric mRNA was identified by high-throughput sequencing of RNA isolated from paraffin-embedded tissue, with TruSeq RNA Exome kit (Illumina) used for the sequencing library construction. A paired-end (2 × 100 bp) run was performed on the NextSeq500 instrument (Illumina) with an average yield of 35 million read pairs and subsequent analysis by alignment to a reference human genome hg38 in a Dragen RNA pipeline (v3.6.3, Illumina). The identified transcript *EWSR1::TFCP2* was validated by reverse transcription–polymerase chain reaction (forward primer—CTGTCCAGGGGTATGGCAC, reverse primer—CCTTCTGTC ATGGAACACCACA) with subsequent Sanger sequencing.

ADDITIONAL INFORMATION

Data Deposition and Access

Consent was obtained to make the patient's or the control's raw DNA or RNA sequencing data publicly available at the European Genome-phenome Archive (EGA) databases (https://ega-archive.org/) under number EGAC00001002710).

Ethics Statement

Written informed consent was obtained from the parents of the individual for participation in the study and the publication. All procedures performed were in accordance with the ethical standards of the institutional and national research committee.

Author Contributions

All authors listed have made a substantial, direct, and intellectual contribution to the work and approved it for publication. A.V.P. performed diagnostics (molecular oncology), analyzed the literature, and wrote and edited the molecular oncology sections. K.Y.S. managed the patient, handled the clinical data, and wrote and edited the clinical sections. M.A.J. managed the patient and handled clinical data. N.Y.U. analyzed the literature and drafted and wrote the manuscript. A.S.S. performed the diagnostics (immunohistochemistry, fluorescence in situ hybridization). V.Y.R. performed the diagnostics (morphology, immunohistochemistry). D.M.K. analyzed the literature and drafted and wrote the pathology sections. A.E.D. analyzed the literature and drafted and wrote the molecular oncology sections.

Competing Interest Statement

The authors have declared no competing interest.

Referees

Patience Obasaju
Charles Keller

Received March 1, 2022; accepted in revised form June 9, 2022.

Funding

The study was supported by Foundation for support and development in the field of pediatric hematology, oncology, and immunology "Science for Children."

REFERENCES

Agaram NP, Zhang L, Sung YS, Cavalcanti MS, Torrence D, Wexler L, Francis G, Sommerville S, Swanson D, Dickson BC, et al. 2019. Expanding the spectrum of intraosseous rhabdomyosarcoma: correlation between 2 distinct gene fusions and phenotype. *Am J Surg Pathol* **43:** 695–702. doi:10.1097/PAS.0000000000001227

Chrisinger JSA, Wehrli B, Dickson BC, Fasih S, Hirbe AC, Shultz DB, Zadeh G, Gupta AA, Demicco EG. 2020. Epithelioid and spindle cell rhabdomyosarcoma with *FUS-TFCP2* or *EWSR1-TFCP2* fusion: report of two cases. *Virchows Arch* **477:** 725–732. doi:10.1007/s00428-020-02870-0

Emami A, Sepehri Z, Gordon JW, Ghavami S. 2017. Biologic and clinical aspects of rhabdomyosarcoma. *Int J Basic Sci Med* **2:** 1–4. doi:10.15171/ijbsm.2017.01

Koutlas IG, Olson DR, Rawwas J. 2021. *FET(EWSR1)-TFCP2* rhabdomyosarcoma: an additional example of this aggressive variant with predilection for the gnathic bones. *Head Neck Pathol* **15:** 374–380. doi:10.1007/s12105-020-01189-1

Le Loarer F, Cleven AHG, Bouvier C, Castex M-P, Romagosa C, Moreau A, Salas S, Bonhomme B, Gomez-Brouchet A, Laurent C, et al. 2020. A subset of epithelioid and spindle cell rhabdomyosarcomas is associated with *TFCP2* fusions and common ALK upregulation. *Mod Pathol* **33:** 404–419. doi:10.1038/s41379-019-0323-8

Lee J, Nguyen PT, Shim HS, Hyeon SJ, Im H, Choi M-H, Chung S, Kowall NW, Lee SB, Ryu H. 2019. EWSR1, a multifunctional protein, regulates cellular function and aging via genetic and epigenetic pathways. *Biochim Biophys Acta Mol Basis Dis* **1865:** 1938–1945. doi:10.1016/j.bbadis.2018.10.042

Lee J, Modave E, Boeckx B, Stacchiotti S, Rutkowski P, Blay JY, Debiec-Rychter M, Sciot R, Lambrechts D, Wozniak A, et al. 2021. Histopathological and molecular profiling of clear cell sarcoma and correlation with response to crizotinib: an exploratory study related to EORTC 90101 "CREATE" trial. *Cancers (Basel)* **13:** 6057. doi:10.3390/cancers13236057

Lewin J, Desai J, Smith K, Luen S, Wong D. 2019. Lack of clinical activity with crizotinib in a patient with FUS rearranged rhabdomyosarcoma with ALK protein overexpression. *Pathology* **51:** 655–657. doi:10.1016/j.pathol.2019.07.004

Li MM, Datto M, Duncavage EJ, Kulkarni S, Lindeman NI, Roy S, Tsimberidou AM, Vnencak-Jones CL, Wolff DJ, Younes A, et al. 2017. Standards and guidelines for the interpretation and reporting of sequence variants in cancer: a joint consensus recommendation of the Association for Molecular Pathology, American Society of Clinical Oncology, and College of American Pathologists. *J Mol Diagn* **19:** 4–23. doi: 10.1016/j.jmoldx.2016.10.002

Lindén M, Thomsen C, Grundevik P, Jonasson E, Andersson D, Runnberg R, Dolatabadi S, Vannas C, Luna Santamaría M, Fagman H, et al. 2019. FET family fusion oncoproteins target the SWI/SNF chromatin remodeling complex. *EMBO Rep* **20:** e45766. doi:10.15252/embr.201845766

Watson S, Perrin V, Guillemot D, Reynaud S, Coindre J-M, Karanian M, Guinebretière JM, Freneaux P, Le Loarer F, Bouvet M, et al. 2018. Transcriptomic definition of molecular subgroups of small round cell sarcomas. *J Pathol* **245:** 29–40. doi:10.1002/path.5053

Willoughby JLS, George K, Roberto MP, Chin HG, Stoiber P, Shin H, Pedamallu CS, Schaus SE, Fitzgerald K, Shah J, et al. 2020. Targeting the oncogene LSF with either the small molecule inhibitor FQI1 or siRNA causes mitotic delays with unaligned chromosomes, resulting in cell death or senescence. *BMC Cancer* **20:** 552. doi:10.1186/s12885-020-07039-1